Conf-950201--15

LA-UR- 95-739

Title: **HIGH STRAIN RATE DEFORMATION OF Ti-48Al-2Cr-2Nb IN THE DUPLEX MORPHOLOGY**

Author(s): **STUART A. MALOY**
GEORGE T. GRAY III

Submitted to: **TMS ANNUAL MEETING**
FEBRUARY 12-16, 1995
LAS VEGAS, NV

Los Alamos
NATIONAL LABORATORY

Form No. 836 R5
ST 2629 10/91

HIGH STRAIN RATE DEFORMATION OF Ti-48Al-2Nb-2Cr IN THE DUPLEX MORPHOLOGY

Stuart A. Maloy and George T. Gray III,

Los Alamos National Laboratory, MST-5, MS-G755, Los Alamos, NM 87545

Abstract

The compressive deformation behavior of Ti-48Al-2Nb-2Cr in the duplex microstructural morphology has been studied at strain rates of 0.001/s and 2000/s over the temperature range from -196 to 1100°C. The material was cast, homogenized, extruded and heat treated to obtain the duplex microstructure. The yield stress is strain rate sensitive at 25°C and increases with temperature at a strain rate of 2000/s from 500 to 1100°C. TEM investigations reveal that deformation occurs in γ-TiAl by means of {111}<112> twinning, 1/2<110> slip, and <101> superdislocations under all conditions depending on the orientation of the grain with respect to the deformation axis. Optical metallography reveals that twinning increases with increasing strain rate. TEM results revealing the dislocation substructure are used to explain the yield stress anomaly.

Introduction

γ-TiAl based materials have received substantial attention recently because of their potential as structural materials for high temperature applications. They have excellent properties compared to existing high temperature alloys because of their low temperature toughness (15-20 $MPam^{1/2}$), high temperature specific strength (comparable to that of nickel superalloys at temperatures up to 700°C), good oxidation resistance and low density (half that of nickel superalloys). Through detailed research on alloy development and property improvement the alloy Ti-48Al-2Nb-2Cr has received attention as a baseline alloy for which a large amount of microstructure/property relationships have been determined [1,2].

γ-TiAl is the major phase in this alloy. γ-TiAl has the $L1_0$ tetragonal crystal structure with lattice parameters, a=0.4005 nm, c=0.4070 nm. The primary modes of deformation for gamma-TiAl are by means of <110> slip, {111}<112> twinning and <101> superdislocations [3]. The secondary phase in Ti-48Al-2Nb-2Cr is Ti_3Al. Ti_3Al has the DO_{19} hexagonal structure with a=0.579 nm and c=0.467 nm. The primary modes of deformation observed in Ti_3Al are prismatic, basal, and pyramidal slip [4].

At temperatures above 25°C and quasi-static strain rates, the yield stress either plateaus or increases with increasing temperature depending on the aluminum content in the material, the heat treatment and the presence of transition metal additions [5-9]. The largest yield stress anomalies have been observed in materials on the Al-rich side of 50Ti-50Al on the phase diagram [7-9], although yield anomalies have also been reported in γ-TiAl alloys on the low aluminum side [6]. Many mechanisms have been postulated to account for this yield stress anomaly in γ-TiAl [10-16]. One theory was proposed to explain a yield stress anomaly observed at 600°C in Ti-54Al [10]. A mechanism similar to Kear-Wilsdorf locking (in $L1_2$ alloys) was proposed in which <101> super dislocations gliding on octahedral (111) planes cross-slip onto cube (010) planes thus becoming locked. This locking mechanism is thermally activated and reaches a maximum at 600°C. Other dislocation locking mechanisms have been proposed by many authors [10-17].

To date, only a limited amount of research has been concerned with the mechanical response of γ-TiAl alloys at high strain rates. Gray [18] has studied the mechanical behavior and resulting deformation substructure of a Ti-48Al-1V alloy at strain rates varying from 0.001 to 7500/s. A rate sensitivity of 0.029 was observed for deformation at room temperature. Harbison, Koss and Bourcier [19] also studied the high strain rate response of the same Ti-48Al-1V alloy at a range of strain rates from 10^{-4}/s to 100/s at room temperature, however, no other tests were performed at other temperatures at high strain rates. Forging of Ti-48Al-2Mn and Ti-48Al has also been performed at strain rates of 0.05/s to 0.5/s at temperatures between 1200 and 1350°C [20] showing these alloys are forgeable at such temperatures. Little other research has been performed on the mechanical properties of γ-TiAl alloys at higher strain rates (>0.1/s).

The purpose of this paper is to report on a study of the mechanical properties of Ti-48Al-2Nb-2Cr heat treated in the duplex microstructure at strain rates of 0.001 to 2000/s and temperatures of -196 to 1100°C. The dislocation and twin substructures are correlated with the mechanical properties.

Experimental Procedure

Ingots of Ti-48Al-2Cr-2Nb (hereafter referred to as Ti-48-2-2) were produced at Dunion Inc. using a vacuum induction skull melting technique [2]. The material was processed as described in reference 2. The analyzed alloy composition in atomic percent was: 48.2% Ti, 47.8% Al, 2.0% Cr, 1.7% Nb, 0.2% 0 and 0.1% C. Trace amounts of interstitials were also present (in wt. ppm): H (17), N (46), and S (10) [2].

Cylindrical specimens 5 mm in length x 5 mm in diameter, were EDM machined for testing with the compression axis cut parallel to the extrusion direction. Quasi-static compression tests at strain rates of 0.001 and 0.1/s were performed at RT and -196°C. Dynamic tests at a strain rate of ~2000/s were conducted at temperatures between RT and 1100°C using a Split-Hopkinson pressure bar [21]. Details of testing are described in reference [18].

Specimens were polished to 0.05 μm alumina paste and etched with Kroll's etchant to reveal deformation twins. TEM samples were polished using conventional procedures to 150 μm and electropolished using a solution of 12 vol.% sulfuric acid and methanol at -20°C to electron transparency.

Results

Initial Microstructure

The starting undeformed duplex microstructure was characterized using optical microscopy and TEM. The duplex microstructure exhibited a grain size ranging from 10 to 100 μm. Optical microscopy of the duplex alloy revealed an inhomogeneous microstructure consisting of small grains with numerous Ti_3Al (α_2) platelets situated on planes perpendicular to the forging direction separating larger TiAl (γ) grains containing a lower amount of α_2. TEM examination revealed a microstructure consisting of small α_2 grains between grains of γ, some grains containing alternating lamella of α_2 and γ and some larger plates of α_2 crossing γ grains. The orientation relationship between the α_2 and γ was identical to that reported previously with $(0001)\alpha_2//\{111\}\gamma$ and $<1120>\alpha_2//<110>\gamma$ [22].

Mechanical testing

The stress/strain response of Ti-48-2-2 tested at -196 and 25°C and strain rates of 0.001, 0.1, and 2000/s is shown in Fig. 1 for the duplex microstructure. The rate sensitivity determined from the flow stress at 2% strain at strain rates of 0.1 and 2000/s is 0.020 at 25°C. The work hardening rate ($d\sigma/d\varepsilon$) notably increases from 2800 to 4500 MPa/unit strain when the strain rate is increased from 0.001 to 2000/s and/or when the test temperature is decreased to -196°C.

An athermal work hardening rate of 4500 MPa/unit strain was observed for the tests performed at 25 to 1100°C. A flow stress anomaly is observed in the duplex alloy (Fig. 2) as the stress at 5% strain decreases with increasing temperature from 25 to 600°C, but then levels off and increases with increasing temperature from 600 to 1100°C. The stress at 5% strain is used to avoid the oscillations in the curve arising from elastic wave dispersion in the pressure bars making accurate yield strength determination difficult. The flow stresses at 10% strain in the duplex alloy are also plotted to show that the work hardening rate is constant and athermal for all the tests performed at a strain rate of 2000/s.

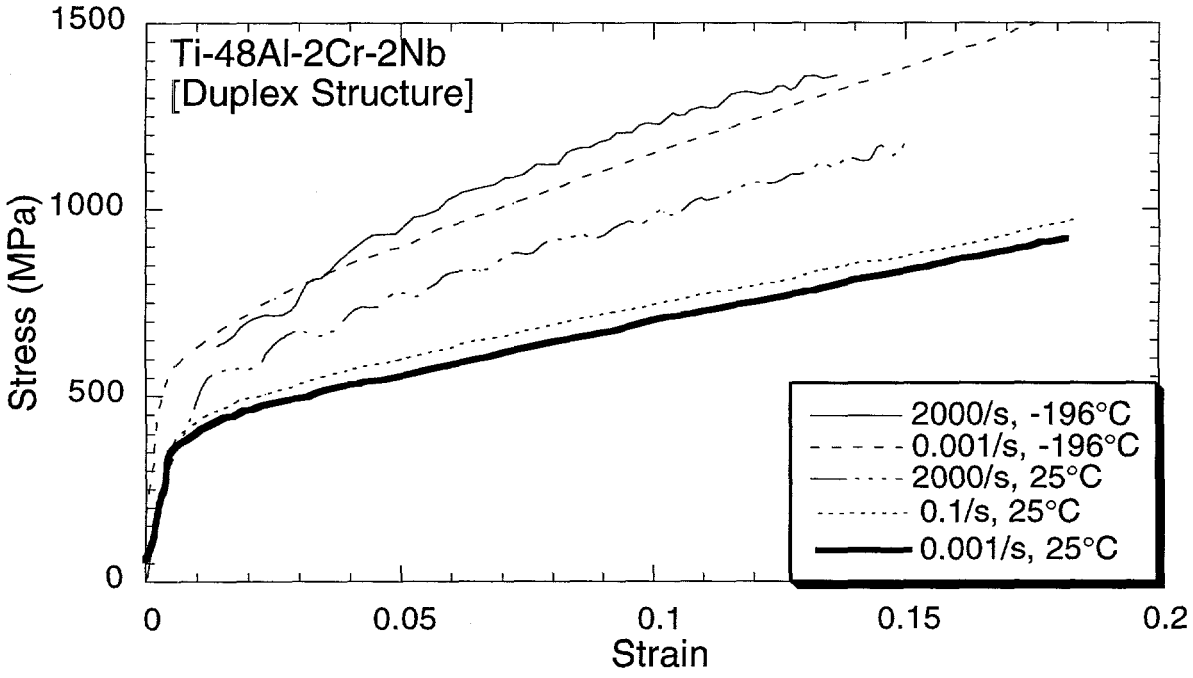

Figure 1 Stress/strain curve for Ti-48Al-2Cr-2Nb in the duplex microstructure tested at RT and -196°C and strain rates of 0.1, 0.001, and 2000/s.

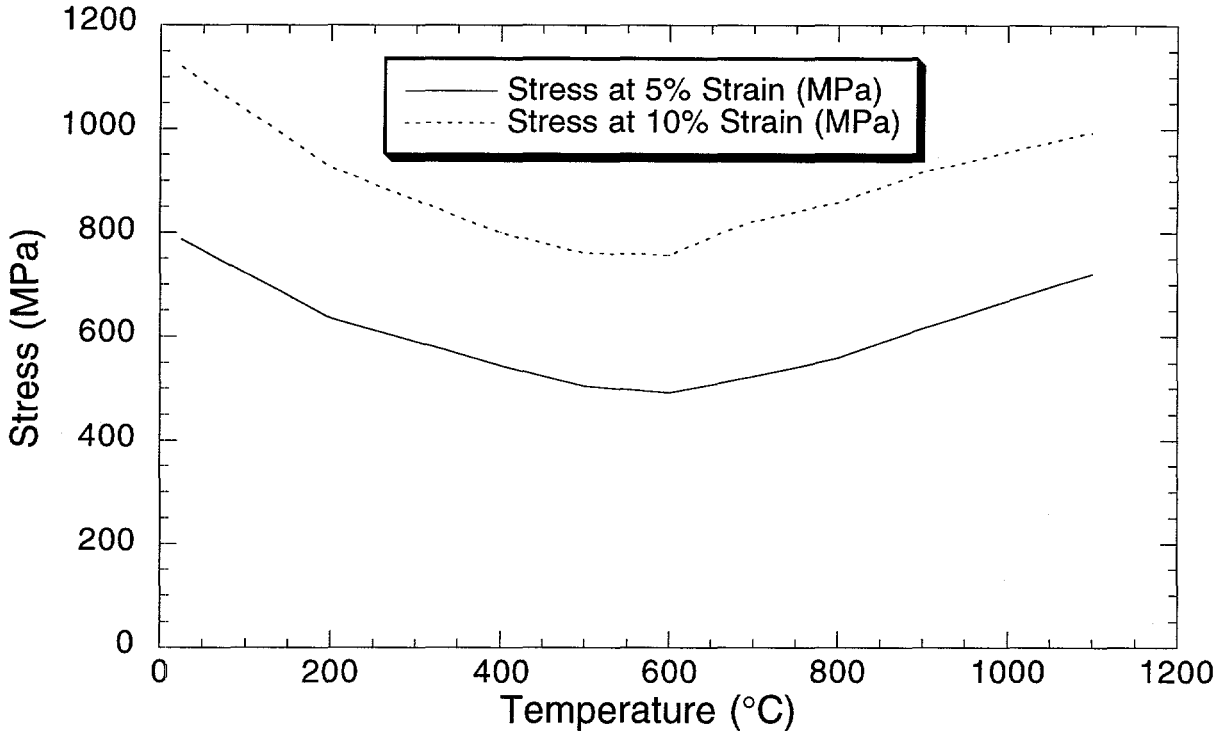

Figure 2 Graph of flow stress vs. temperature for Ti-48Al-2Cr-2Nb tested at a strain rate of 2000/s and temperatures ranging from RT to 1100°C.

TEM

In all of the TEM foils observed after deformation to a plastic strain of 12-18%, different deformation substructures were observed among different grains. Some grains exhibited twinning and 1/2<110> dislocations while others deformed via <101> superdislocations and 1/2<110> dislocations. After deformation at all temperatures at a strain rate of 2000/s, planar slip was observed in the α_2. Although, distinct changes in the dislocation substructure were observed with increasing temperature. The major differences observed in the TEM foils were are described below. An in depth description of the TEM study will be published at a later date.

After deformation at room temperature and 2000/s, twins in γ grains were often observed crossing planar laths of α_2 causing an offset in the α_2 lath. In γ grains which did not deform by twinning, the deformation substructure consisted of 1/2<110> dislocations and curved <101> superdislocations. The curved superdislocations are evident in a weak beam dark field micrograph imaging with g=(002) as shown in Fig. 3.

Following deformation at 400°C, twinning was still observed in packets which upon intersecting α_2 laths, caused shear offsets. In γ grains which did not deform by twinning, <101> dislocations were beginning to lie along screw orientations. The 1/2<110> dislocations were bowed and intersected the <101> superdislocations.

Pure screw <101> superdislocations and 1/2<110> dislocations intersecting the <101> superdislocations were observed after deformation at 900°C and a strain rate of 2000/s in the γ-grains deformed by slip. A detailed g.b analysis (to be published later) revealed long straight [101] dislocations (marked A in Fig. 4) and [101] dislocations (marked B in Fig. 4). The superdislocations were observed separated into partials as shown in the weak beam dark field micrograph in the inset of Fig. 4.

Optical Metallography

After prestraining at a strain rate of 0.001/s at 25 and -196°C and a strain rate of 2000/s at 25, 400 and 900°C, samples were polished and etched using Kroll's etchant. Two major differences were observed when comparing the samples tested at strain rates of 0.001 and 2000/s

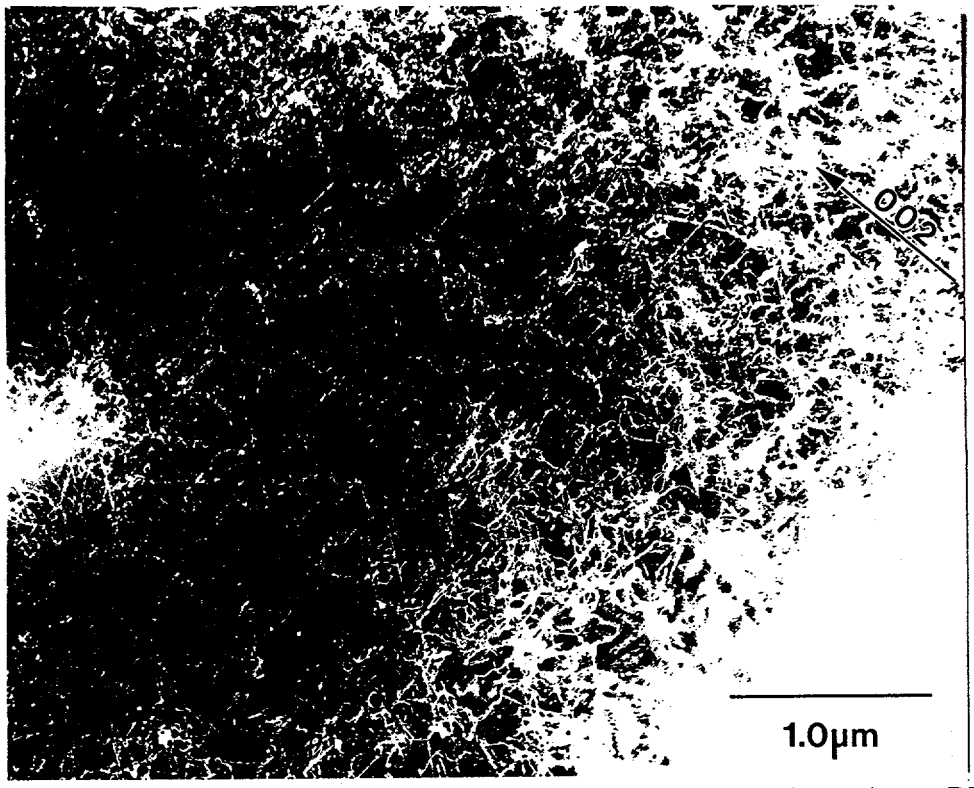

Figure 3 TEM micrograph showing curved superdislocations after deformation at RT and a strain rate of 2000/s

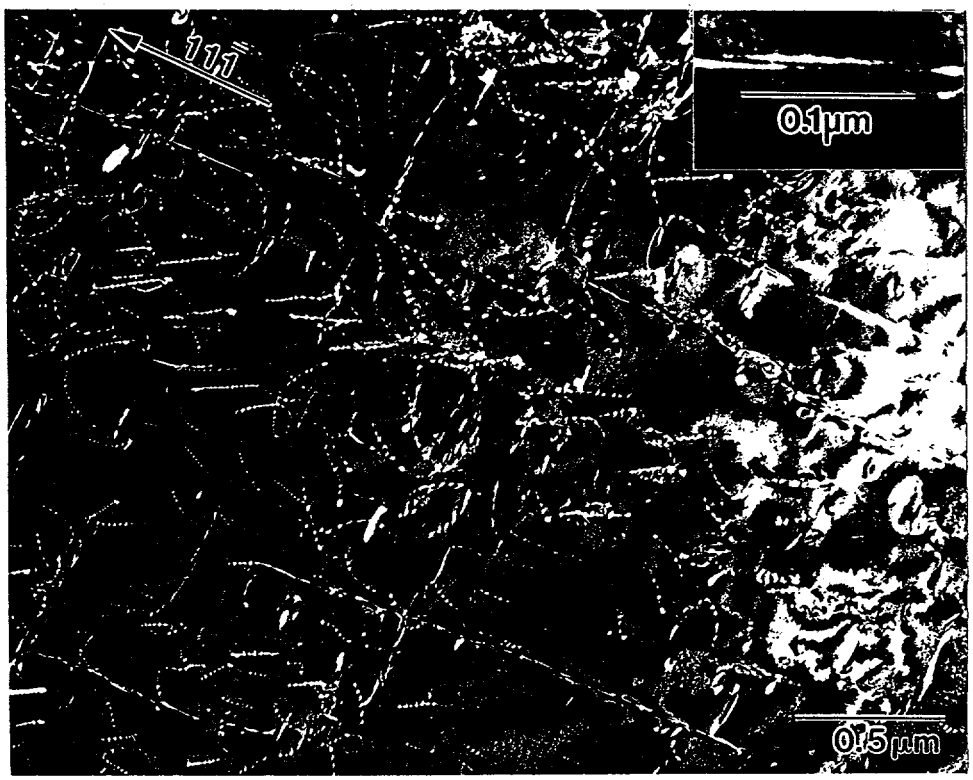

Figure 4 Weak beam dark field TEM micrograph showing <101> pure screw superdislocations (marked A and B) after deformation at 900°C and a strain rate of 2000/s. Inset shows superdislocations separated into partials

Figure 5 Dark field optical micrographs showing deformation twins formed from (a) deformation at RT and a strain rate of 0.001/s and (b) deformation at RT and a strain rate of 2000/s.

at 25°C as shown in the optical dark field micrographs of Fig. 5 (a and b). First, a slight increase in twinning is observed following prestraining at high strain rate. Second, twinning occurs on multiple variants within one grain when deformed at a strain rate of 2000/s and is usually on a single variant within one grain when deformed at 0.001/s. This evidence was also confirmed by TEM.

Discussion

There are three modes of deformation in TiAl: {111}<112> twinning, {111}1/2<110> slip and {111}<101> slip. In this study, the configuration of dislocations gliding in the {111}<101> slip system was studied in detail, because of the strong role the <101> superdislocations play in controlling the yield stress anomaly [8,9]. <101> superdislocations were curved after deformation at 25°C and a strain rate of 2000/s while they became straight along their screw orientation after deformation at 400°C and above. Previous detailed weak beam studies [10,11] have shown that <101> superdislocations cross-slip onto {010} planes resulting in a peak in the yield stress at a temperature of 600°C at low strain rate. Similar to the Kear-Wilsdorf mechanism in Ni_3Al, the cross-slipped segments pin the dislocations and cause the yield stress to increase. In this study, the change in configuration of the <101> superdislocations with increasing temperature suggests that these <101> dislocations cross-slip on {010} planes and become pinned, resulting in an increased forest dislocation density which interacts with the 1/2<110> dislocations and pins the <101> dislocations. At slow strain rates (0.001/s), enough time is allowed for the <101> superdislocations to unlock themselves by thermal activation. Thus, the flow stress decreases with temperature above 600°C. On the other hand, at a strain rate of 2000/s, insufficient time is allowed for climb to occur and therefore the flow stress continues to rise at temperatures up to 1100°C. Previous work has shown that the yield stress of polycrystalline Ni_3Al (with 0.095 at.% boron) tested at a strain rate of 3000/s also continues to increase even up to a temperature of 1000°C [22].

The effect of increasing strain rate on deformation in Ti-48-2-2 is illustrated in the stress/strain response as well as the resulting deformation substructure. The main difference in the stress/strain response is an increase in the work hardening rate from 2800 to 4500 MPa/unit strain

with increasing strain rate from 0.001 to 2000/s. The cause of this increasing work hardening rate is found in the deformation substructure.

The deformation substructure reveals that slip is planar in the α_2 at high strain rates resulting from the reduced amount of cross-slip [24]. In addition, in the γ grains, more twinning and twinning on multiple variants in one grain is observed after deformation at a strain rate of 2000/s. The reduced amount of cross-slip will not allow dynamic recovery of dislocations to occur, and the twinning on multiple variants within one grain affects subsequent storage of forest dislocations. Each of these factors would lead to a higher work hardening rate.

In comparison with the results of Gray [18] on high strain rate testing of Ti-48Al-1V, a similar rate sensitivity was observed at room temperature (0.029) for that alloy to that observed for the duplex Ti-48-2-2 alloy (0.020). A yield stress anomaly was not observed in this previous work, although the yield stress began to plateau at 600°C and testing was not performed above 700°C. Therefore, a yield stress anomaly may have been present if testing were performed at temperatures above 700°C. In addition, because of the high carbon content of the Ti-48Al-1V alloy used, the yield stress was ~100 MPa greater than that observed for the duplex γ-alloy in this study. Alternatively, the strengthening obtained from the carbon addition in the Ti-48Al-1V may have partially masked the yield stress anomaly.

Conclusions

1) The mechanical properties of the Ti-48Al-2Cr-2Nb investigated in this study in a duplex microstructure have been measured at strain rates of 0.001, 0.1 and 2000/s at temperatures from -196 to 1100°C.
2) The rate sensitivity was determined to be 0.020 at 25°C over strain rate range from 0.1 to 2000/s.
3) An increase in the strain rate causes an increase in the work hardening rate from 2800 to 4500 MPa/unit strain at 25°C.
4) As the strain rate is increased an increase in the overall twinning propensity and multiple twin variants were seen to be activated in each grain as observed optically and using TEM.
5) As the temperature is increased from -196°C to 1100°C at a strain rate of 2000/s, a yield stress anomaly is observed with a minimum yield stress occurring at ~500°C.
6) Observation of the deformation substructure after testing revealed that <101> dislocations were curved after deformation at 25°C and a strain rate of 2000/s while they were pinned in the screw orientation after deformation at temperatures above 400°C resulting in the yield stress anomaly.

Acknowledgments:

The authors acknowledge the technical assistance of Robert Carpenter II and Michael F. Lopez in performing the mechanical property measurements. This work was performed under the auspices of the U.S. Department of Energy.

References

1. Huang, S-C, U.S. patent 4,879,092 (1989).

2. Shih, D.S., Huang, S-C., Scarr, G.K., Jang, H. and Chesnutt, J.C., in Microstructure/Property Relationships in Titanium Alloys and Titanium Aluminides, Ed. by Y-W Kim and R.R. Boyer, TMS, Pittsburgh, pp. 135-148, (1991).

3. Lipsitt, H.A., Shechtman, D., and Schafrik, R.E., Metall. Trans. A, p. 1991, (1975).

4. Court, S.A., Lofvander, P.A., Loretto, M.H., and Fraser, H.L., Phil. Mag. A, 61[1], pp. 109-139, (1990).

5. Kandra, J.T. and Lee, E.W., Met. and Mat. Trans. A, 25A, pp. 1667-1679, (1993).

6. Morris, M.A., Phil. Mag. A, 69[1], 129-150, (1994).

7. Huang, S-C., and Hall, E.L., Met. Trans.A, 22A, pp. 427-438, (1991).

8. Whang, S.H. and Hahn, Y.D., Scripta Metall. and Mater., 24, pp. 485-490, (1990).

9. Stucke, M.A., Vasudevan, V.K., and Dimiduk, D.M., Mater. Sci. and Engrg., in press, (1994).

10. Hug, G., Loiseau, A., and Veyssiere, P., Phil. Mag. A, 57[3], 499-523, (1988).

11. Morris, M.A. and Lipe, T., Scripta Metall. et Mater., 31[6], 689-694, (1994).

12. Court, S.A., Vasudevan, V.K. and Fraser H.L., Phil. Mag. A, 61[1], 141-158, (1990).

13. Greenburg, B.A., Antonova, O.V., Indenbaum, V.N., Karkina, L.E., Notkin, A.B., Ponomarev, M.V., and Smirnov, L.V., Acta metall. and mater., 39[2], 233-242, (1991).

14. Kawabata, T., Kanai, T. and Izumi, O., Phil. Mag. A, 63[6], 1291-1298, (1991).

15. Kawabata, T., Kanai, T. and Izumi, O., Acta Metall., 33[7], 1355-1366, (1985).

16. Hahn, Y.D. and Whang, S.H., Scripta Metall. and Mater., 24, pp. 139-144, (1990).

17. Greenberg, B.A., Scripta Met., 23, 631-636, (1989).

18. Gray G.T. III, in Microstructure/Property Relationships in Titanium Alloys and Titanium Aluminides, ed. by Y-W. Kim and R.R. Boyer, TMS, Warrendale, Pa, pp. 263-274, (1991).

19. Harbison, L.S., Koss, D.A., and Bourcier, R.J., in Titanium'92, Science and Technology, Ed. by F.H. Froes and I. Caplan, TMS, Warrendale, PA, pp. 1661-1667, (1993).

20. Zhang, X.D., Ramanujan, R.V., Dean, T.A., Dewes, R., Jacobs, M.H. and Wise, M.L.H., in Titanium'92, Science and Technology, Ed. by F.H. Froes, and I. Caplan, TMS, Warrendale, PA, pp. 1107-1090, (1993).

21. C.E. Frantz, P.S. Follansbee, and W.J. Wright, in High Energy Rate Fabrication, ed. by I. Berman and J.W. Schroeder, (NY: Amer. Soc. Mech. Engr.), p. 229, (1984).

22. Blackburn, M.J., The Science Technology and Application of Titanium, (Oxford: Pergamon Press), p. 633, (1970).

23. Sizek, H.W., and Gray III, G.T., Acta metall. mater., 41[6], pp. 1855-1860, (1993).

24. Gray, George T. III, in " Modeling of Crystalline Solids, ed. by T.C. Lowe, A.D. Rollett, P.S. Follansbee, G.S. Daehn, TMS, Warrendale, PA, pp. 145-158, (1991).